Permeation of Phenol through Ethylene Copolymer Hollow Fibers

A. Keith Fritzsche[a]

[a] MONSANTO TRIANGLE PARK DEVELOPMENT, CENTER RESEARCH TRIANGLE PARK, NORTH CAROLINA

PLEASE SCROLL DOWN FOR ARTICLE

Permeation of Phenol through Ethylene Copolymer Hollow Fibers

A. KEITH FRITZSCHE

MONSANTO TRIANGLE PARK DEVELOPMENT CENTER
RESEARCH TRIANGLE PARK, NORTH CAROLINA 27709

Abstract

Hollow fibers were spun from low-density polyethylene, an ethylene/propylene copolymer, ethylene/vinyl acetate copolymers, and ethylene/ethyl acrylate copolymers. The phenol permeation rates through these hollow fibers by reactive dialysis were measured over a range of temperatures, allowing the calculation of the apparent activation energies for transport. The permeation rates for phenol transport were found to be dependent upon the degree of crystallinity in the hollow fiber and the increased solubility of phenol in the hollow fiber due to the presence of the polar ethyl acrylate and vinyl acetate groups in the amorphous phase.

INTRODUCTION

Recovery of phenol from industrial waste streams has become increasingly desirable for two reasons. First, the concerns for the environment have generated ever-increasing pressure to prevent discharge of toxic chemicals. Second, discarding phenol represents a costly loss of a valuable raw material.

It is well known that the composition of a liquid mixture, such as a waste stream, can be altered by allowing a portion of the mixture to permeate through a polymeric membrane. This phenomenon provides a basis for a separation process and has motivated a substantial amount of research and development effort in recent years. Numerous approaches have been taken to remove phenol from water via membranes. Representative of those approaches are reverse osmosis (1–3), solvent extraction (4), and reactive dialysis (5–7).

In reactive dialysis, a phenol-laden waste stream and a sweep stream

1323

are separated by a semipermeable membrane through which phenol transport occurs. The phenol permeates across the membrane and enters the sweep stream. The phenol concentration in the sweep stream is maintained near zero by chemically converting the phenol by reaction with sodium hydroxide to the ionized, nonpermeating sodium phenate. Phenol may then be recovered from the concentrated sweep stream, and the processed stream should have a sufficiently low phenol concentration for safe discharge to the environment.

Polyethylene is permeable to phenol (*8*). Low-density polyethylene is a suitable hollow fiber material because it is chemically resistant to attack by phenol and caustic (*9*). It has acceptable physical strength, is permeable to phenol, and yet is impermeable to sodium phenate. The work described here concerns hollow fibers from low-density polyethylene as well as those from selected ethylene copolymers which could also be fabricated as hollow fibers for this separation. These copolymers possess acceptable physical and chemical properties and yield higher phenol permeabilities than those found in low-density polyethylene hollow fibers.

THEORY

The fundamental differential equation of diffusion, known as Fick's law, is

$$\frac{\delta c}{\delta t} = \frac{\delta}{\delta x} D\left[\frac{\delta c}{\delta x}\right] \tag{1}$$

which was derived by assuming that the flux of a substance is proportional to the concentration gradient measured normal to the section. The proportionality coefficient is called the diffusivity, D, and is one of the fundamental properties of the system. The units of D are $(length)^2/time$, e.g., cm^2/sec.

Another fundamental parameter of the system is the solubility, S. All diffusing species will have a finite solubility in the polymer membrane. As is the case of the diffusion coefficient, the solubility is a function of the transporting species and the properties of the polymer.

Permeability is dependent upon the solubility of the permeant in the membrane as well as its diffusion through the membrane. Permeability, P, may be expressed by

$$P = DS \tag{2}$$

The temperature dependence of the permeability coefficient over moderate temperature ranges can be represented by an Arrhenius-type equation:

$$P = P_0 \exp\left(-E_p/RT\right) \tag{3}$$

where $P = DS$, $P_0 = D_0 S_0$, and E_p is the apparent activation energy for permeation equal to the sum of the apparent activation energy for diffusion, E_d, and the heat of solution, H_s. The derivations of these equations are presented in detail in the literature (10).

For acceptable permeation rates to be achieved, the permeant must diffuse rapidly through the membrane and it must be highly soluble in the membrane. At the same time, increased solubility of the permeant in the membrane causes it to swell and lose its physical properties. These phenomena present a dilemma, frequently encountered in the application of membranes for industrial processes, which must be overcome in order to achieve a practical separation system.

EXPERIMENTAL

Materials

The polymer resins used in this study were all commercially available. Film-grade resins were used whenever possible to minimize gel content in the resin. The resins used in this investigation are listed in Table 1.

Melt Spinning Process

The hollow fibers were spun using conventional melt spinning techniques. The following procedure as practiced by Fritzsche and Leonard

TABLE 1

Composition and Melt Indices of Resins Used

Resin[a]	Composition		Melt index
	% Ethylene	% Comonomer	
1	100	0	2.65
2	92	8 VA[b]	7.0
3	88	12 VA	2.5
4	82	18 VA	8.0
5	92	8 EA[c]	8.0
6	85	15 EA	1.5
7	81	19 EA	6.0
8	65–60	35–40 P[d]	—

[a]Resins 1–4 are Alathon polymers manufactured by E. I. du Pont de Nemours; Resins 5–7 are products of Union Carbide, and Resin 8 is manufactured by Exxon.
[b]VA is vinyl acetate.
[c]EA is ethyl acrylate.
[d]P is propylene.

is illustrative of these techniques (7). The polymer pellets were fed by gravity into a Brabender 3/4 in. extruder with a metering pump to control the melt pressure on the spinnerette assembly. The spinnerettes were the tube-in-orifice type, with the inner tube connected to a low-pressure nitrogen supply. The nitrogen pressure was controlled by a bubble tube immersed in either silicone oil or $ZnCl_2$ in water. Sand pack filters or porous metal filter cartridges were used between the metering pump and the spinnerette. The spinnerette assembly was controlled independently by an electrically heated jacket to maintain a constant temperature as measured by a thermocouple inserted in the spinnerette assembly. The filaments were collected on an adjustable speed take-up within a range of 50 to 1200 ft/min.

The quenching of the extruded fibers may be delayed by maintaining a heated environment about them for a brief period after their extrusion from the spinnerette assembly. This has been accomplished by passing the fibers through a chimney or jacket after exiting the spinnerette for a short distance prior to their exit to air or liquid quenching, i.e., cooling. The chimney is a cylindrical jacket of 6 in. to 2 ft in length, with an inside diameter equal to or larger than the diameter of the spinnerette, and it is provided with heating means adapted to maintain a wall temperature somewhat above the operating temperature of the spinnerette. After exiting from the chimney the fibers are quenched or cooled by passage through an area of ambient room temperature air for a sufficient distance to cool and thoroughly solidify the hollow fibers.

The size and wall thickness of the hollow fibers produced can be controlled in several ways. Initially, the size of the orifice, tube, and inert gas pressure selected will govern the size of fibers produced, as modified by the degree of enlargement of fiber dimensions by release from the metered pressure of extrusion through the spinnerette. Size and wall thickness can be varied by varying the pressure of extrusion through the spinnerette and the take-up speed at which the fibers are drawn away from the spinnerette. Changes in one of these values can be compensated for by changes in the other. Once solidification has been achieved, it is possible to draw the hollow fibers to reduce the wall thickness, but such procedures were not used in these experiments because of the additional crystallization of the polymeric material in the hollow fibers thereby induced.

Fiber Testing

The fibers were tested and evaluated according to the techniques described in detail in U.S. Patent 4,082,658 (7). They were skeined into test loops usually containing 60 fibers per loop. The loops were then

preannealed in water for 1 hr at the maximum temperature at which they were to be tested. The loops were preannealed while unrestrained to permit relaxation of orientation. These loops were then potted into test cells using an epoxy resin, as shown in Fig. 1. The portion of the test cell below the rubber stopper was exposed to a stirred, thermostatted 1% phenol/water bath at the temperature of interest. The volume of this bath was sufficiently large so that little change occurred in its measured phenol concentration throughout the duration of each test. The rubber stopper was used for mounting the test cell in the support above the bath. The fiber arms were used for the introduction or collection of the bore fluid.

EPOXY

SUMP EXIT
(NaOH + NaOφ)

PVC NIPPLE

NaOH
SUMP
ENTRANCE

EPOXY TUBESHEET

RUBBER STOPPER

PVC SHELL

INTERFACIAL REGION
(ZONE BETWEEN TUBESHEET
AND ACTIVE REGION)

HOLLOW FIBERS

ACTIVE REGION
(EXPOSED PORTION OF
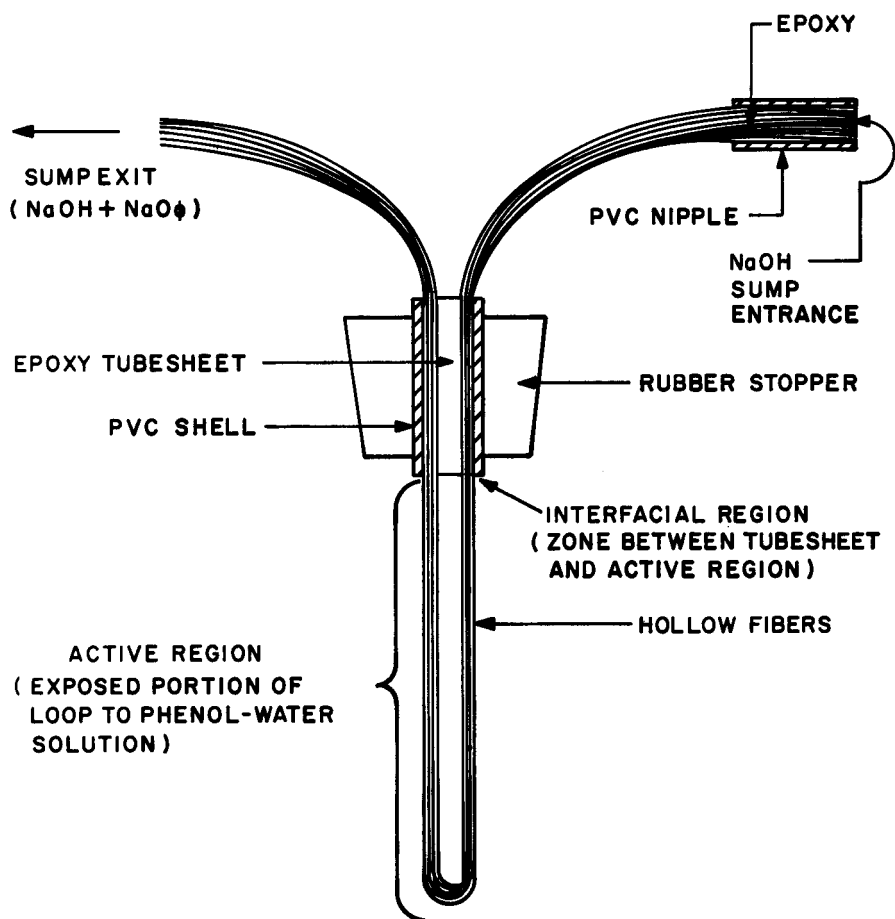LOOP TO PHENOL-WATER
SOLUTION)

FIG. 1. Diagram of 3/8 in. test cell.

The permeation rates were determined by continually pumping dialysis fluid (15% NaOH in water) through the bore for at least 1 hr from a caustic reservoir. The phenol-laden bore effluent was collected and quantitatively transferred to a volumetric flask for dilution to a given volume. The amount of phenol transported across the hollow fiber wall per unit time was calculated from the amount of sodium phenate in the effluent and the duration of the test. Measurement of the sodium phenate concentration was made from its absorption in the ultraviolet at 287 mμ on a Cary 11 recording spectrophotometer. Multiple test cells were used in each measurement, and less than a 10% variation was found in the calculated permeability results.

Data Treatment

The permeation rate of the fibers was calculated from the sodium phenate concentration by

$$P_A = \frac{J_{ID}}{\Delta V} = \frac{CW_1/W_2}{At\Delta V} \qquad (4)$$

where P_A = net permeation rate, cm^3/cm^2-sec-ΔV

$\quad\quad J_{ID}$ = the flux of phenol through the wall of the hollow fiber based on the inner diameter, g/cm^2-sec

$\quad\quad \Delta V$ = volume fraction of phenol in the feed assuming unit density

$\quad\quad C$ = measured sodium phenate concentration in grams

$\quad\quad W_1$ = formula weight of phenol

$\quad\quad W_2$ = formula weight of sodium phenate

$\quad\quad A$ = total internal area of the exposed regions of the hollow fibers, cm^2

$\quad\quad t$ = time of exposure in seconds

The intrinsic permeability, P, of the hollow fibers is calculated from P_A by

$$P = (P_A)\frac{ID}{2} \ln\left(\frac{OD}{ID}\right) \qquad (5)$$

where P = intrinsic permeability, (cm^3-cm)/(sec-cm^2-ΔV)

$\quad\quad ID$ = internal hollow fiber diameter, cm

$\quad\quad OD$ = external hollow fiber diameter, cm

The intrinsic permeability is a measure of the inherent permeability of the hollow fiber material. However, J_{ID} as well as P_A are inversely proportional to the wall thickness. Therefore, it is desirable to reduce the wall

thickness as much as possible to increase the flux of phenol for a material of given intrinsic permeability while maintaining sufficient physical properties in the fiber.

RESULTS AND DISCUSSION

The intrinsic permeabilities of the hollow fibers spun from a series of ethylene/vinyl acetate copolymers were measured over a temperature range of 30 to 70°C. These results, as well as those obtained from low-density polyethylene hollow fibers, are given in Table 2. Semilogarithmic plots were made of the intrinsic permeability versus the reciprocal of the absolute temperature. A series of straight lines resulted as shown in Fig. 2. The Arrhenius equation was used to estimate the apparent activation energy for transport (E_p) and the Arrhenius contant (P_0). These values for E_p and P_0 are also given in Table 2. The apparent activation energy for transport is found to be inversely proportional to the vinyl acetate content.

Similar increases in permeability were observed with a series of hollow fibers spun from ethylene/ethyl acrylate copolymers. These results are given in Table 3.

Hollow fibers were also spun from an ethylene/propylene thermoplastic rubber which contained 35 to 40 wt-% propylene and 60 to 65 wt-% ethylene. The resultant hollow fibers were quite rubbery, possessing high elongation, low tensile strength, and high elastic recovery upon heating the drawn fiber. The degree of crystallinity in this fiber was much less than that in the other fibers studied. The permeation rates were measured at a series of temperatures. These intrinsic permeabilities and the calculated Arrhenius constants are shown in Table 4.

In all of the copolymer systems studied, the hollow fibers possessed

TABLE 2

Phenol Permeability as a Function of Percent Vinyl Acetate and Temperature

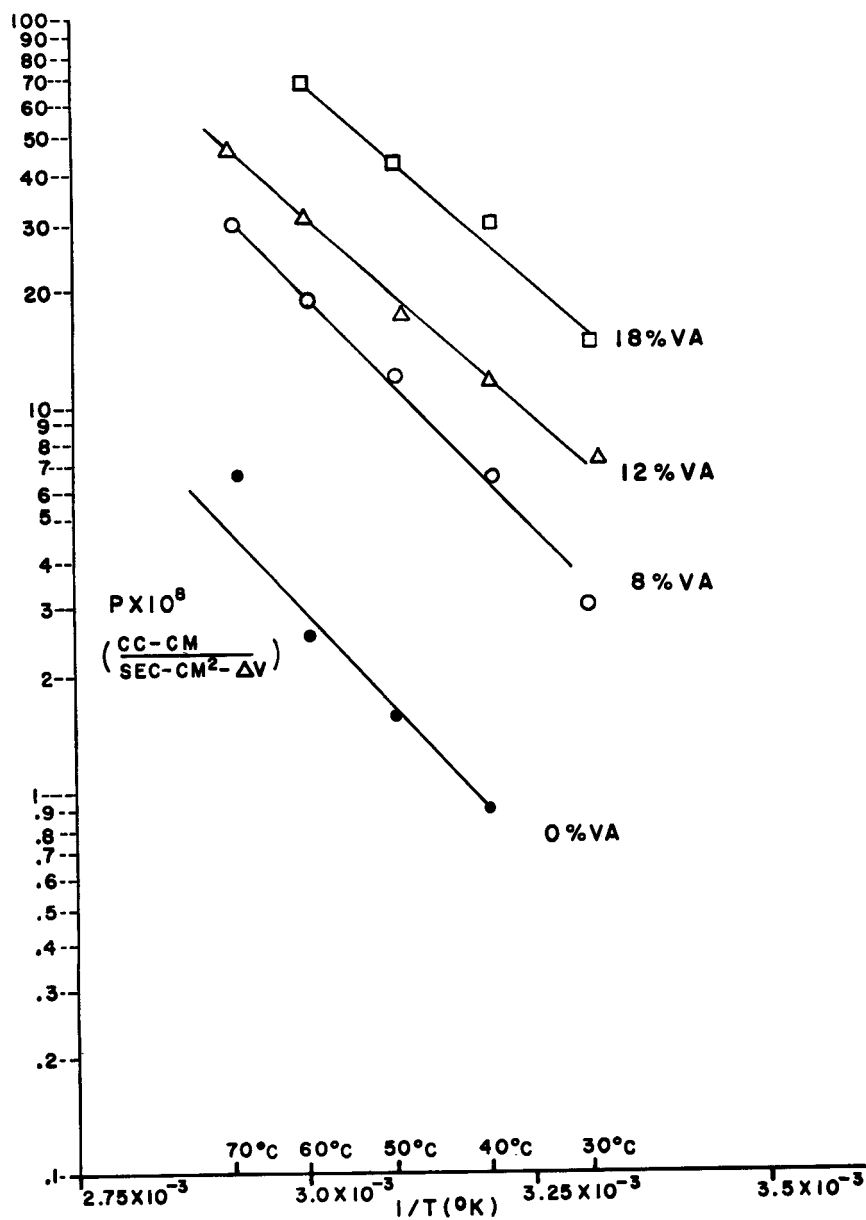|	$P \left[\dfrac{cm^3\text{-}cm}{sec\text{-}cm^2\text{-}\Delta V} \right] \times 10^8$ for resin (wt-% VA) of			
Temperature (°C)	0	8	12	18
30	—	3.0	7.1	15
40	0.9	6.5	11.5	30
50	1.6	11.6	17.8	43
60	2.6	18.7	30.0	67
70	5.8	30.4	46.0	—
E_p (kcal/mole)	11.6	11.0	9.7	9.6
$P_0 \left[\dfrac{cm^3\text{-}cm}{sec\text{-}cm^2\text{-}\Delta V} \right]$	1.17	3.02	0.66	1.37

FIG. 2. Variation of permeability with temperature of ethylene copolymers containing increasing amounts of vinyl acetate.

TABLE 3

Phenol Permeability as a Function of Weight Percent Ethyl Acrylate

Temperature (°C)	$P \left[\frac{cm^3\text{-}cm}{sec\text{-}cm^2\text{-}\Delta V} \right] \times 10^8$ for resin (wt-% EA) of			
	0	8	15	19
60	2.6	16	—	45
70	5.8	25	59	—

TABLE 4

Permeation Rates of Phenol through Ethylene Propylene
Thermoplastic Rubber with Temperature[a]

Temperature (°C)	$P \left[\frac{cm^3\text{-}cm}{sec\text{-}cm^2\text{-}\Delta V} \right] \times 10^8$
50	6.0
60	9.0
70	22
80	27

[a] $P_0 = 10.77 \left[\frac{cm^3\text{-}cm}{sec\text{-}cm^2\text{-}\Delta V} \right]$

$E_p = 12.2$ kcal/mole

higher phenol permeation rates than those observed with the low-density polyethylene hollow fibers.

On factor contributing to the higher phenol permeation rates in the copolymer hollow fibers is the reduction of the degree of crystallinity in the hollow fiber as the comonomer content increases. The decrease in crystallinity with increasing vinyl acetate content has been measured. Nielsen showed that the percent crystallinity at 30°C decreased from 57 to 29.5% as the vinyl acetate content increased from 0 to 18.77 wt-% (11). Salyer and Kenyon also showed that the crystallinity of the polyethylene is reduced in proportion to the molar concentration of comonomer (12).

The crystalline regions in the polymer influence the permeability. The solubility of the permeant is directly proportional to the noncrystalline content because the crystalline regions act as impermeable filler. The crystalline regions also reduce the diffusion rate of the permeant through the polymer because they increase the tortuosity of the diffusion path and act as giant cross-linking agents which restrict the mobilities of the neighboring chain segments. The effects of these factors have been developed and discussed in considerable detail (12–21).

However, the decrease in the degree of crystallinity is not the only

factor which contributes to the enhanced phenol permeability of the ethylene/vinyl acetate and ethylene/ethyl acrylate copolymer hollow fibers. The ethylene/propylene thermoplastic rubber hollow fiber had the lowest degree of crystallinity seen in any of the hollow fibers studied, as can be seen by ranking the hollow fibers by their elastic moduli measured via the Vibron in 3% phenol/water at 70°C. The elastic modulus of the ethylene/propylene thermoplastic rubber hollow fiber of $E = 0.24 \times 10^8$ dyn/cm^2 was well below those of the other hollow fibers measured, such as $E = 6.4 \times 10^8$ dyn/cm^2 for the polyethylene hollow fiber and 3.1×10^8 dyn/cm^2 for the 12% vinyl acetate-containing hollow fiber. Yet the ethylene/propylene thermoplastic rubber hollow fiber had the lowest phenol permeabilities of any of the copolymer hollow fibers measured at any studied temperature.

It is apparent that the enhanced phenol permeability of the vinyl acetate- and ethyl acrylate-containing copolymers over the propylene-containing copolymer results from the enhanced solubility of phenol in the membrane due to the incorporation of these polar monomers into the polymer chain.

Michaels and co-workers observed that the liquid flux rates through polypropylene films depended primarily upon the solubility of the permeants in the films, and the absolute difference in the solubility parameters of the polymer–liquid pair provided a good basis for correlation of this effect. As seen in Table 5, the solubility parameters of polyvinyl acetate and polyethyl acrylate are closer to phenol than are those of polyethylene, polypropylene, or ethylene/propylene copolymers. One would expect that as the amounts of vinyl acetate or ethyl acrylate are increased in a copolymer with ethylene, the solubility parameter of the resultant copolymer would change. The solubility parameter would increase from 7.9 for the polyethylene to 9.4 for the polyvinyl acetate and polyethyl acrylate. During this process, regions of high phenol solubility would occur in the noncrystalline regions of the copolymer hollow fiber due to the presence of the vinyl acetate and ethyl acrylate monomers. Because the permeability

TABLE 5

Solubility Parameters of Polymers and Phenol

	δ	Refs.
Phenol	14.5	23
Polyethylene	7.9	24, 25
Polypropylene	8.1	22
Ethylene propylene rubber	7.9	26
Polyvinyl acetate	9.4	27, 28
Polyethyl acrylate	9.4	28–30

is a product of the diffusion and solubility, a higher permeability will result. Furthermore, the solubility is described by an Arrhenius-type equation. The logarithms of the permeability versus the mole percent comonomer content yielded the expected straight lines, shown in Fig. 3, for the permeabilities measured at 60 and 70°C. Furthermore, since polyvinyl acetate and polyethyl acrylate have the same solubility parameters, the data points representing these copolymers fall on the same lines. However, it is obvious that neither of these straight lines intersects the measured permeabilities of the low density polyethylene hollow fibers when extrapolated to zero comonomer concentration. The crystallites formed in the ethyl acrylate and vinyl acetate copolymers are primarily composed of ethylene units. The ethyl acrylate and vinyl acetate units exist primarily in the amorphous regions. Consequently, the molar concentration of vinyl acetate and ethyl acrylate units in the amorphous regions is greater than that suggested by the overall copolymer composition. If the degree of crystallinity were measured directly in these hollow fibers, the molar content of comonomer could be calculated. Since these data were not available, the comonomer molar contents in the amorphous phase were estimated using the data obtained by Nielsen on vinyl acetate copolymers (11). Two assumptions were made in these calculations. First, it was assumed that the crystallinities in Nielsen's samples were identical to those in the hollow fibers. However, he used different ethylene/vinyl acetate copolymers, and melt spinning of the materials into hollow fibers can yield a different structural morphology. Second, it was assumed that comparable results exist for the ethyl acrylate copolymer system. The logarithms of the permeability were plotted against the estimated mole percent of comonomer in the amorphous phase. Straight lines resulted which, when extrapolated to zero comonomer content, intersected the ordinate near the measured permeability values of the low-density polyethylene hollow fibers, as shown in Fig. 4. For instance, the measured permeabilities of the polyethylene hollow fibers are 2.6×10^{-8} and 5.8×10^{-8} at 60 and 70°C, respectively. The permeability values resulting from extrapolation to zero comonomer content are 4.1×10^{-8} and 6.2×10^{-8} at these same temperatures.

CONCLUSIONS

The permeation rates of phenol through ethylene copolymer hollow fibers are controlled primarily by the comonomer content and the degree of crystallinity. The degree of crystallinity in the hollow fiber is reduced as increasing amounts of propylene, ethylene acrylate, and vinyl acetate are incorporated into the polymer chain. However, higher phenol permea-
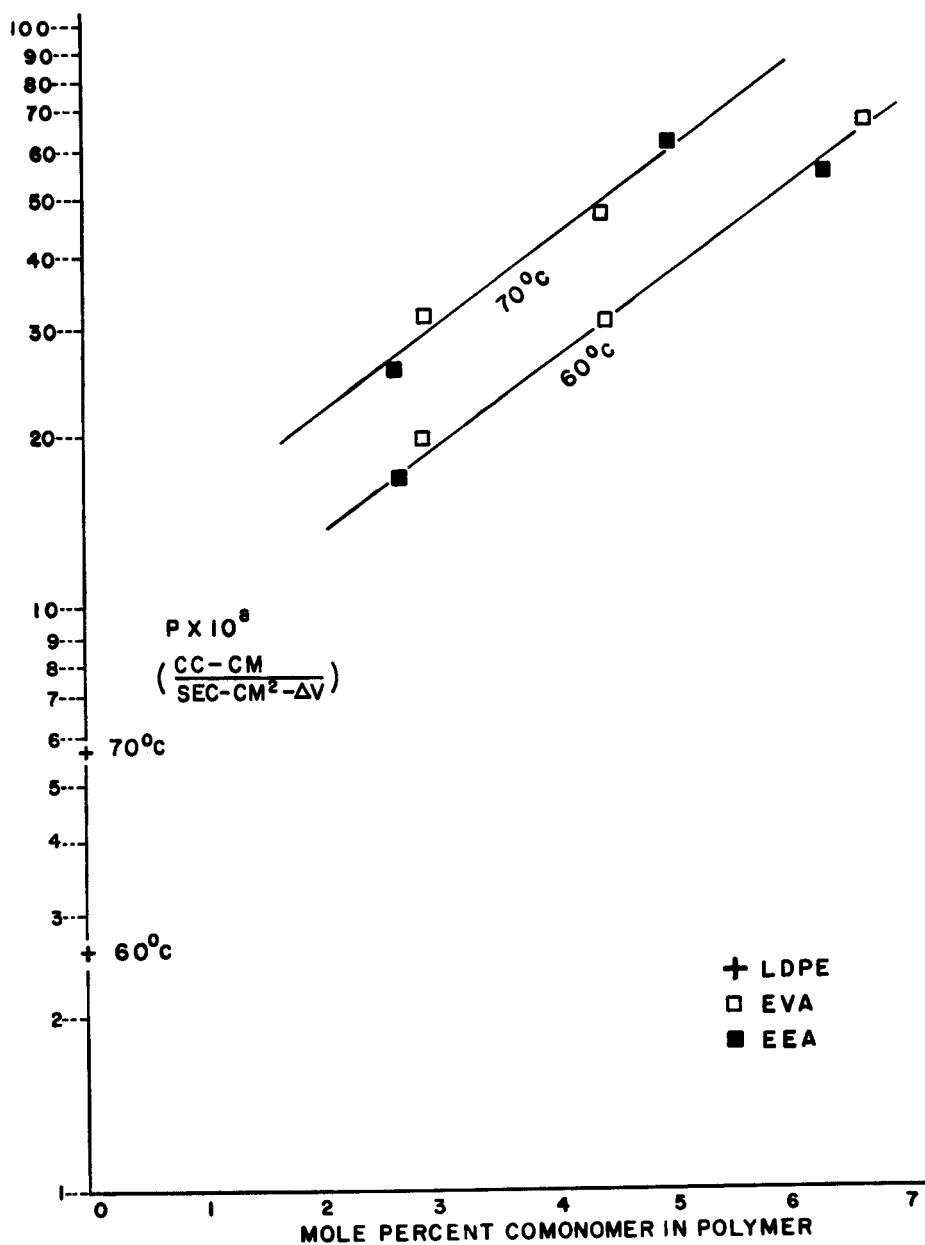
FIG. 3. Logarithms of phenol permeability at 60 and 70°C as a function of
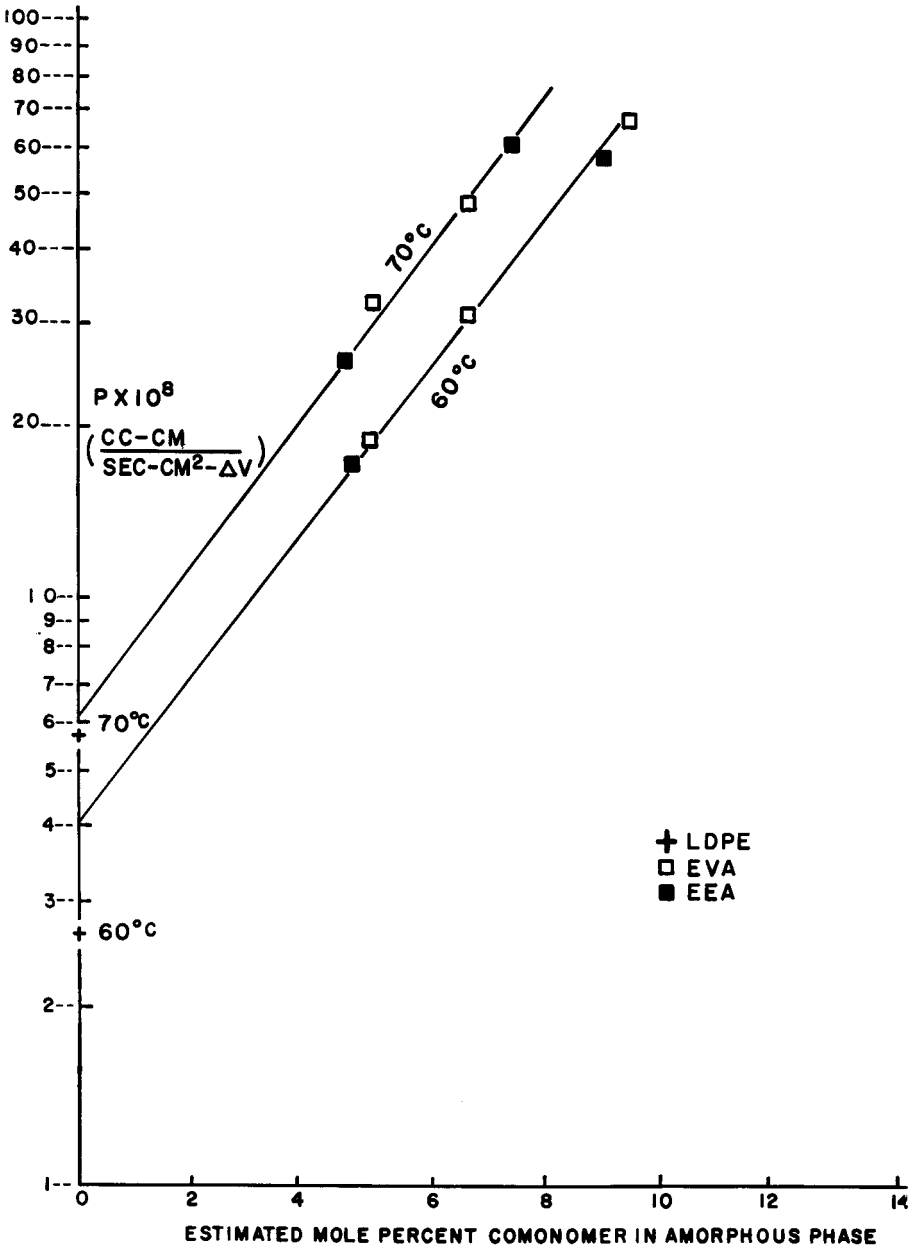mole percent comonomer.

FIG. 4. Logarithms of phenol permeability at 60 and 70°C as a function of estimated mole percent comonomer in amorphous phase.

bilities were observed in hollow fibers spun from ethylene/vinyl acetate and ethylene/ethyl acrylate copolymers than were observed with the ethylene/propylene copolymer hollow fibers which possessed the lowest degree of crystallinity. These higher rates apparently result from the presence of the polar ethyl acrylate and vinyl acetate units. These units appear to enhance the solubility of the phenol in the amorphous phase, yielding much higher phenol transport rates than would be expected from the reduction of crystallinity alone.

Acknowledgments

REFERENCES

1. H. K. Lonsdale, U. Merten, and M. Tagami, *J. Appl. Polym. Sci.*, *11*, 1807 (1967).
2. T. Matsuura and S. Sourirajan, *Ibid.*, *15*, 2905 (1971).
3. T. Matsuura and S. Sourirajan, *Ibid.*, *16*, 2531 (1972).
4. L. T. C. Lee, W. Ho, and K. Liu, U.S. Patent 3,956,112 (1976).
5. E. Klein, J. K. Smith, R. E. C. Weaver, R. P. Wendt, and S. V. Desai, *Sep. Sci.*, *8*, 585 (1973).
6. C. E. Hamilton, U.S. Patent 3,931,000 (1976).
7. A. K. Fritzsche and R. L. Leonard, U. S. Patent 4,082,658 (1978), Belgian Patent 863,764 (1978).
8. M. Salame, *SPE Trans.*, p. 153 (1961).
9. E. Perry, British Patent 1,480,018 (1977).
10. J. Crank and G. S. Park (eds.), *Diffusion in Polymers*, Academic, London, 1968.
11. L. E. Nielsen, *J. Polym. Sci.*, *42*, 357 (1960).
12. I. O. Salyer and A. S. Kenyon, *J. Polym. Sci., Part A-1*, *9*, 3083 (1971).
13. C. E. Rogers (ed.), *Permselective Membranes*, Dekker, New York, 1971.
14. P. Meares, *Polymers; Structure and Bulk Properties*, Van Nostrand, London, 1965.
15. V. Stannett, M. Szwarc, R. L. Bhargava, J. A. Meyer, A. W. Myers, and C. E. Rogers, *Permeability of Plastic Films and Coated Papers to Gases and Vapors*, TAPPI Monograph 23, New York, 1962.
16. C. H. Klute and P. Franklin, *J. Polym. Sci.*, *32*, 161 (1958).
17. C. H. Klute, *J. Appl. Polym. Sci.*, *1*, 340 (1959).
18. C. H. Klute, *J. Polym. Sci.*, *41*, 307 (1959).
19. A. S. Michaels and R. B. Parker, *Ibid.*, *41*, 53 (1959).
20. A. S. Michaels and H. J. Bixler, *Ibid.*, *50*, 393 (1961).
21. A. S. Michaels and H. J. Bixler, *Ibid.*, *50*, 413 (1961).
22. A. S. Michaels, W. Vieth, A. S. Hoffman, and H. A. Alcaloy, *J. Appl. Polym. Sci.*, *13*, 577 (1969).
23. M. Guinot, *Genie Chim.*, *85*, 85 (1961).
24. M. Magat, *J. Chim. Phys.*, *46*, 344 (1949).
25. R. B. Richards, *Trans. Faraday Soc.*, *42*, 20 (1946).
26. T. J. Dudek and F. Bueche, *J. Polym. Sci.*, *2A*, 812 (1963).
27. P. A. Small, *J. Appl. Chem.*, *3*, 71 (1953).

28. G. Allen, *Polymer*, *2*, 375 (1961).
29. D. Mangaraj, S. Petra, and S. Rashid, *Makromol. Chem.*, *65*, 29 (1963).
30. D. Mangaraj, S. Petra, and S. B. Bath, *Ibid.*, *67*, 75 (1963).